Journal of Zhejiang University-SCIENCE B 2026 27(8):872-887
www.jzus.zju.edu.cn; www.springer.com/journal/11585
E-mail: jzus_b@zju.edu.cn

Research Article
https://doi.org/10.1631/jzus.B2500237

Check for updates

Neuroprotection of engineered *Clostridium butyricum*-pMTL007-GLP-1 in A53T α-synuclein (α-syn) mouse model via PI3K/AKT/GSK-3β

Xin FANG[1,3,5,6*], Yun WANG[1,3,5,6*], Zhenli LONG[4], Bin LIAO[1,3,5,6], Bo WANG[1,3,5,6], Daojun HONG[1,3,5,6], Jie LUO[7✉], Tingtao CHEN[1,2✉]

[1]*Department of Neurology, The First Affiliated Hospital, Jiangxi Medical College, Nanchang University, Nanchang 330006, China*
[2]*Jiangxi Province Key Laboratory of Bioengineering Drugs, School of Pharmacy, Jiangxi Medical College, Nanchang University, Nanchang 330031, China*
[3]*Institute of Neurology, Jiangxi Academy of Clinical Medical Science, The First Affiliated Hospital, Jiangxi Medical College, Nanchang University, Nanchang 330006, China*
[4]*School of Queen Mary, Nanchang University, Nanchang 330031, China*
[5]*Rare Disease Center, The First Affiliated Hospital, Jiangxi Medical College, Nanchang University, Nanchang 330006, China*
[6]*Key Laboratory of Rare Neurological Diseases of Jiangxi Provincial Health Commission, Jiangxi Medical College, Nanchang University, Nanchang 330006, China*
[7]*School of Public Health, Jiangxi Medical College, Nanchang University, Nanchang 330031, China*

Abstract: Parkinson's disease (PD) is a prevalent neurodegenerative disorder with limited therapeutic options and no cure, underscoring the urgent need for novel treatment strategies. Our previous work demonstrated that an engineered strain of *Clostridium butyricum*-pMTL007-glucagon-like peptide-1 (*C. butyricum*-pMTL007-GLP-1) alleviated PD symptoms by enhancing mitophagy, though the exact molecular mechanisms remained incompletely understood. In this study, we further investigated the neuroprotective effects and underlying mechanisms of this engineered strain using an A53T α-synuclein (α-syn) transgenic mouse model of PD. Specifically, we evaluated its impact on motor function, gut α-syn expression, intestinal barrier function, gut microbial composition, and neuropathological changes, with a focus on the phosphoinositide-3-kinase (PI3K)/protein kinase B (AKT)/glycogen synthase kinase-3β (GSK-3β) signaling pathway. Our findings revealed that *C. butyricum*-pMTL007-GLP-1 ameliorated motor deficits in PD mice by reducing intestinal α-syn accumulation, restoring gut barrier function, and modulating microbial diversity—notably increasing the relative abundance of *Prevotella* at the genus level. Furthermore, the engineered strain attenuated neuropathological alterations by decreasing phosphorylated α-syn (p-α-syn) in the substantia nigra while upregulating tyrosine hydroxylase (TH), dopamine-transporter (DAT), and glucagon-like peptide-1-receptor (GLP-1R) expression. These neuroprotective effects were associated with suppressed proinflammatory responses and enhanced anti-inflammatory and anti-apoptotic signaling, likely mediated through PI3K/AKT/GSK-3β pathway activation. In conclusions, *C. butyricum*-pMTL007-GLP-1 exerts significant neuroprotective effects in PD mice by reshaping gut microbiota composition and activating the PI3K/AKT/GSK-3β pathway. These findings provide further theoretical support for the potential application of probiotic-based therapies in PD treatment.

Key words: Parkinson's disease; Glucagon-like peptide-1 (GLP-1); *Clostridium butyricum*-pMTL007-GLP-1; Gut microbiota; PI3K/AKT/GSK-3β pathway

1 Introduction

Parkinson's disease (PD) is a progressive neurodegenerative disorder characterized by four cardinal motor symptoms: resting tremor, bradykinesia, muscle rigidity, and postural instability. The disease's neuropathological hallmarks include the accumulation of misfolded α-synuclein (α-syn) aggregates, progressive degeneration of dopaminergic neurons in the substantia

✉ Jie LUO, jieluo@ncu.edu.cn
Tingtao CHEN, chentingtao1984@163.com
* The two authors contributed equally to this work
Jie LUO, https://orcid.org/0000-0002-1501-9922
Tingtao CHEN, https://orcid.org/0000-0002-0506-8536

Received May 9, 2025; Revision accepted July 21, 2025; Crosschecked June 16, 2026; Published online June 27, 2026

nigra pars compacta, and the formation of intraneuronal Lewy bodies (Mulvaney et al., 2020; Tripodi et al., 2024). Epidemiologically, PD affects approximately 1% of the global population over 60 years of age, with prevalence increasing dramatically to 3%–4% among octogenarians. This represents a growing public health challenge with substantial socioeconomic implications (Tarsy, 2012). Despite decades of research, PD remains a complex multifactorial disorder whose exact etiopathogenesis continues to elude complete understanding (Lv et al., 2020). Current gold-standard pharmacotherapies, principally Levodopa, dopamine-receptor agonists, and monoamine-oxidase-B inhibitors, offer primarily symptomatic relief by targeting dopaminergic pathways but fail to modify the underlying disease progression (Chang et al., 2022). This critical therapeutic gap underscores the pressing need to develop novel treatment strategies that can both alleviate symptoms and fundamentally alter the neurodegenerative course of PD, thereby improving long-term patient outcomes and quality of life.

Current evidence highlights the critical role of the phosphoinositide-3-kinase (PI3K)/protein kinase B (AKT) signaling pathway in PD, where it regulates cell survival and modulates inflammatory responses (Malagelada et al., 2008; Yang et al., 2014). Downstream of this pathway, glycogen synthase kinase-3β (GSK-3β) drives α-syn aggregation and neuroinflammation. Its activity is regulated through inhibitory phosphorylation at Ser9 (Kozikowski et al., 2006; Golpich et al., 2015), with accumulating studies implicating GSK-3β as a key contributor to PD pathogenesis (Lei et al., 2011). Pharmacological interventions targeting GSK-3β have demonstrated therapeutic potential. For instance, chlorogenic acid reduces rotenone-induced phosphorylated α-syn levels by inhibiting GSK-3β activity. Similarly, PNU-120596 attenuates neuroinflammation in murine models by suppressing the Janus kinase 2 (JAK2)/nuclear factor-κB (NF-κB)/GSK-3β axis (Gowayed et al., 2022; Sharma et al., 2022). These findings suggest that modulating GSK-3β to enhance PI3K/AKT signaling represents a promising strategy for PD treatment.

Glucagon-like peptide-1 (GLP-1), a gut-derived hormone secreted by intestinal L cells, and its receptor agonists (such as exendin-4) have demonstrated well-documented neuroprotective effects in multiple rodent models of PD (Holst, 2007; Hölscher, 2018; Reich and Hölscher, 2022). Mechanistically, GLP-1 receptor (GLP-1R) activation initiates PI3K/AKT signaling through its canonical G-protein-coupled receptor (GPCR) pathway involving sequential β-arrestin recruitment, adenylate cyclase stimulation, and protein kinase A (PKA)-dependent PI3K activation. This signaling cascade's critical role in GSK-3β modulation has been consistently demonstrated across multiple disease models (Alzheimer's disease (AD), PD, and trophoblasts), with PI3K inhibitors reliably abolishing these effects (Meng et al., 2016; Yang et al., 2016; Wang et al., 2018; Wu et al., 2018). However, the therapeutic application of GLP-1 is severely constrained by rapid enzymatic degradation once in the bloodstream, resulting in an extremely short half-life of merely 1–2 min (Lorenz et al., 2013). While synthetic GLP-1 analogs have been developed to circumvent this limitation, their clinical utility remains hampered by the necessity for prolonged subcutaneous administration and high treatment costs, which collectively diminish patient compliance and impose significant socioeconomic burdens. Consequently, developing strategies to improve the pharmacokinetic and pharmacoeconomic profile of GLP-1-based therapies represents a critical unmet need in PD treatment.

Emerging evidence underscores the potential of microbial interventions in promoting healthy aging, with particular emphasis on the gut microbiota's pivotal role in PD pathogenesis (Wang et al., 2021; Chidambaram et al., 2022; Xu et al., 2024; Liu et al., 2025). Preclinical investigations and clinical observations have consistently shown that probiotic administration can effectively modulate the gut microbiota, strengthen intestinal barrier integrity, and attenuate neuroinflammatory responses, consequently mitigating PD-related symptoms (Snigdha et al., 2022). A notable example is *Clostridium butyricum*, which has been demonstrated to improve motor dysfunction in PD murine models through the gut microbiota-GLP-1 signaling axis (Sun et al., 2021). Nevertheless, large-scale, well-controlled clinical trials remain imperative to conclusively validate the therapeutic efficacy of probiotics and elucidate their precise mechanisms of action in PD management.

In our previous studies, we successfully developed two genetically engineered strains, *Lactococcus lactis* MG1363-pMG36e-GLP-1 and *Escherichia coli* Nissle 1917-GLP-1, both of which demonstrated significant

neuroprotective effects in murine models of PD (Fang et al., 2020; Wu et al., 2023). *C. butyricum*, a generally recognized as safe (GRAS)-certified strain, outperforms *E. coli* (virulence risks) and *Lactobacillus* (low transformation efficiency, 1×10^4–1×10^5 colony-forming units (CFU)/μg DNA) with its gastric acid resistance (>90% survival), superior intestinal colonization (1×10^8 CFU/g), and high transformation efficiency (1×10^7 CFU/μg DNA). Its therapeutic potential in PD further supports its use as an ideal engineered probiotic vector (Stoeva et al., 2021; Sun et al., 2021; Zhang et al., 2024). Building upon these findings, we subsequently engineered the *C. butyricum*-pMTL007-GLP-1 strain. This novel construct combines the neuroprotective properties of GLP-1 with the therapeutic potential of *C. butyricum* and has shown promising neuroprotective outcomes in 1-methyl-4-phenyl-1,2,3,6-tetrahydropyridine (MPTP)-induced PD mouse models (Wang et al., 2023). While these results are encouraging, the exact molecular mechanisms mediating these neuroprotective effects remain to be fully elucidated. In the current study, we employed a well-characterized A53T α-syn transgenic PD mouse model to systematically evaluate the therapeutic potential of *C. butyricum*-pMTL007-GLP-1. Our comprehensive approach combines behavioral assessments, molecular analyses, and gut microbiota profiling to uncover the underlying mechanisms of action. We anticipate that this study will provide valuable mechanistic insights and robust experimental evidence to advance PD therapeutics, potentially contributing to the development of next-generation engineered bacterial medications.

2 Materials and methods

2.1 Animals and experimental design

Thirty-two 2-month-old male A53T α-syn transgenic mice and eight wild-type C57BL/6 mice were purchased from Changzhou Cavens Laboratory Animal Co., Ltd. (Changzhou, China) and maintained under specific pathogen-free (SPF) conditions with controlled environmental parameters (12 h:12 h light-dark cycle, 50%–55% humidity, 22–24 °C) and ad libitum access to food and water. All experimental procedures were conducted at 9:00–12:00 a.m. to minimize circadian variability (see treatment schedule in Fig. 1a). Following a 6-month acclimatization period (from 2 to 8 months of age), we confirmed successful model establishment through standardized behavioral assessments. Wild-type C57BL/6 mice (n=8, Group C) received daily oral gavage of 100 μL gelatin-saline solution (0.1% (1 g/L) gelatin in 0.9% (9 g/L) saline) for 30 d, while the transgenic mice were randomly divided into four treatment groups (n=8 per group). The AM group (disease model) received daily oral gelatin-saline (100 μL); the AL group (positive control) received daily intraperitoneal injections of 0.4 mg/kg liraglutide (GLP-1R agonist) to circumvent potential oral degradation; the ACB group received daily oral administration of 1×10^8 CFU/mL *C. butyricum* in 0.01% gelatin-saline (100 μL); and the ACBG group received equivalent dosing of *C. butyricum*-pMTL007-GLP-1 via identical administration protocol. All animal procedures strictly adhered to National Institutes of Health (NIH) guidelines and were approved by the Animal Experimental Ethical Inspection Committee of Nanchang Royo Biotechnology Co., Ltd., Nanchang, China (Approval No. RyE2021070912).

2.2 Behavioral assessment

All mice were habituated to the behavioral chamber environment for 30 min 24 h prior to testing. Behavioral assessments were then conducted following established protocols from our previous study (Wang et al., 2023). These included three standardized tests: (1) the pole test involved a cotton-wrapped vertical pole (50 cm in length, 1 cm in diameter), with descent time (from top to base) recorded as the primary outcome measure; (2) the open-field test took place in a 40 cm×40 cm arena where total distance traveled and central zone exploration (20 cm×20 cm center area) were automatically tracked over a 10 min session using video analysis software (ANY-maze V6.3, Stoelting Co., USA), and the arena was wiped with 70% (volume fraction) ethanol between trials; (3) the hanging wire test evaluated neuromuscular coordination with mice positioned on a suspended wire (50 cm in length, 2 mm in diameter) and scored limb engagement (0–4 points based on number of paws maintaining grip, with immediate 0 score upon falling). All tests were performed in a dedicated behavioral suite with 15 min inter-test intervals to minimize stress interference, and final scores represented the mean of three consecutive trials per animal conducted on separate days to ensure reliability.

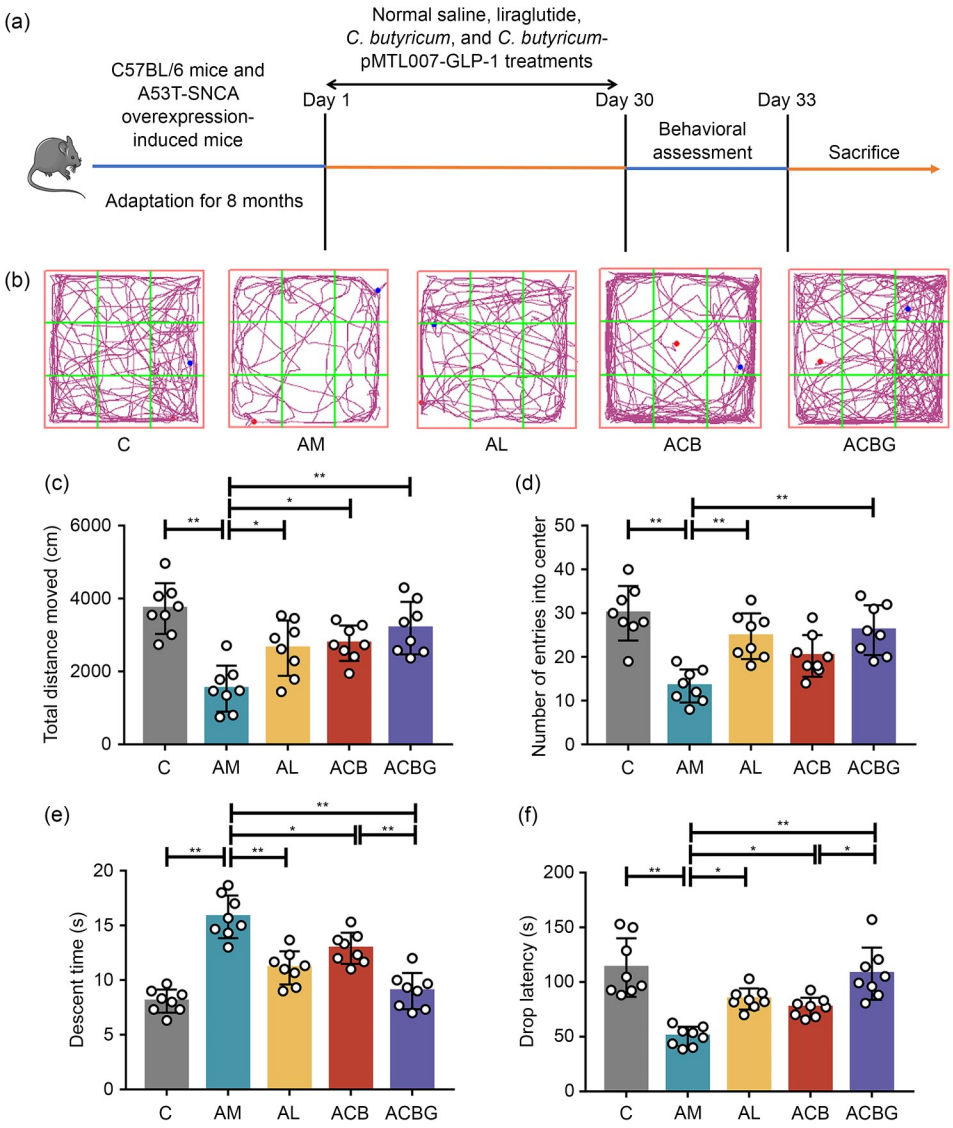

Fig. 1 ***Clostridium butyricum*-pMTL007-glucagon-like peptide-1 (*C. butyricum*-pMTL007-GLP-1) alleviated motor abnormalities in Parkinson's disease (PD) mice. (a) Schematic diagram of the experimental design. (b) Movement trajectories of the five groups of mice in the open-field test. The blue dot indicates the starting point, and the red dot indicates the endpoint. (c) Cumulative distance traveled in the open-field test. (d) Number of entries into the center in the open-field test. (e) Descent time in the pole test. (f) Drop latency in the hanging wire test. Data were analyzed by one-way analysis of variance (ANOVA) with Tukey's post hoc test for multiple comparisons. Data are presented as mean±standard deviation (SD). * P<0.05, ** P<0.01. C: normal mice (n=8); AM: PD mice (n=8); AL: liraglutide-treated PD mice (n=8); ACB: *C. butyricum*-treated PD mice (n=8); ACBG: *C. butyricum*-pMTL007-GLP-1-treated PD mice (n=8).**

2.3 Sample collection

Following behavioral assessment, mice were humanely euthanized via isoflurane overdose. Blood samples were collected via cardiac puncture, allowed to coagulate at 37 °C for 2 h, and then centrifuged at 3000*g* for 15 min at 4 °C to obtain serum, which was aliquoted and stored at −80 °C until analysis. Fresh fecal pellets were immediately flash-frozen in liquid nitrogen and maintained at −80 °C for subsequent 16S ribosomal RNA (rRNA) sequencing and microbiota profiling. Brain tissues (including substantia nigra and striatum) and intestinal segments (duodenum, jejunum, and colon) were either snap-frozen in liquid nitrogen for molecular analyses or immersion-fixed in 4% (0.04 g/mL) paraformaldehyde (PFA) in 0.1 mol/L phosphate buffer (pH 7.4) for 24 h at 4 °C before paraffin embedding and histological processing.

2.4 Gut microbiota analysis

Gut microbiota composition was analyzed using 16S rRNA high-throughput sequencing following established protocols (Chen et al., 2018). Genomic DNA was extracted from the mouse fecal samples and subjected to polymerase chain reaction (PCR) amplification targeting the V3–V4 hypervariable regions of the 16S rRNA gene using universal primers 338F (5'-ACTCCTACGGGAGGCAGCAG-3') and 806R (5'-GGACTACHVGGGTWTCTAAT-3'; where H=A/T/C, V=G/A/C, and W=A/T) (Personalbio, Shanghai, China). We sequenced the resulting amplicons on an Illumina platform to generate raw sequencing data, which were subsequently processed through the QIIME2 pipeline (version 2019.4). Sequence analysis was performed using the UPARSE software package, and sequences sharing ⩾97% similarity were clustered into operational taxonomic units (OTUs). Following OTU clustering, read counts were normalized by rarefaction to the minimum sequencing depth across all samples to ensure comparability. Alpha diversity metrics were then calculated to assess microbial community complexity. We taxonomically classified representative sequences from each OTU, based on alignment with the Ribosomal Database Project (RDP) reference database. The resulting species-abundance matrix was used for downstream analyses. All sequencing data were deposited in the NCBI sequence read archive under accession No. PRJNA1091924.

2.5 Immunofluorescence and immunohistochemistry

Brain and colon tissues were embedded in paraffin and sectioned into 5 μm thick slices. Following deparaffinization and rehydration, endogenous peroxidase activity was blocked by incubating the sections with 3% (volume fraction) H_2O_2, followed by blocking with 5% (0.05 g/mL) goat serum at room temperature. The sections were then incubated overnight at 4 ℃ with primary antibodies (Table S1). After washing, bound primary antibodies were detected using corresponding secondary antibodies. Immunoreactivity was visualized under a light microscope (Nikon Eclipse Ci, Nikon Corporation, Japan) (Higashi et al., 2007).

2.6 Western blot analysis

Brain and colon tissues were homogenized in radioimmunoprecipitation assay (RIPA) lysis buffer (Solarbio Life Science, China, Cat. No. R0010) containing protease and phosphatase inhibitors to preserve protein integrity during extraction. Following homogenization, lysates were centrifuged at 12 000*g* for 10 min at 4 ℃, and the resulting supernatants were collected for protein quantification using a bicinchoninic acid (BCA) assay kit (Thermo Fisher Scientific, Cat. No. A53226). Equal amounts of protein were resolved by 10%–12% (0.10–0.12 g/mL) sodium dodecyl sulfate-polyacrylamide gel electrophoresis (SDS-PAGE) and electrophoretically transferred onto polyvinylidene fluoride (PVDF) membranes. After blocking with 5% (0.05 g/mL) non-fat milk in Tris-buffered saline containing 0.1% (0.001 g/mL) Tween-20 (TBST) for 1 h at room temperature, membranes were probed overnight at 4 ℃ with primary antibodies (Table S1). Following three washes with TBST, membranes were incubated with horseradish peroxidase (HRP)-conjugated secondary antibodies diluted in 1% (volume fraction) milk-TBST for 1 h at room temperature. Protein-antibody complexes were visualized using an enhanced chemiluminescence (ECL) detection system (Thermo Fisher Scientific, USA), and band intensities were quantified by densitometric analysis using ImageJ software (NIH, USA) (Zeng et al., 2017).

2.7 Quantitative real-time PCR

Total RNA was isolated from brain tissue using TRIzol reagent (Invitrogen, USA) and reverse-transcribed into complementary DNA (cDNA) using a PrimeScript RT reagent kit (TaKaRa, Japan, Cat. No. 639506). Quantitative real-time PCR (qRT-PCR) was performed on an ABI 7900HT Fast Real-Time PCR system (Applied Biosystems, USA) using SYBR Green chemistry. Each 20 μL reaction mixture contained: 10 μL of 2× SYBR Premix EX Taq II, 0.4 μL of ROX Reference Dye II (50×) (TaKaRa, Japan, Cat. No. RR420A), 1.0 μL of cDNA template, 0.8 μL each of forward and reverse primers (final concentration 0.4 μmol/L), and 7 μL of nuclease-free water. The thermal cycling protocol consisted of an initial denaturation at 95 ℃ for 10 min, followed by 40 cycles of 95 ℃ for 30 s, 60 ℃ for 30 s, and 72 ℃ for 30 s. Gene expression levels of target genes (interleukin-1β (*IL-1β*), *IL-6*, tumor necrosis factor-α (*TNF-α*), and *GLP-1R*) were normalized to the endogenous control glyceraldehyde 3-phosphate dehydrogenase (GAPDH) and calculated using the comparative threshold cycle ($2^{-\Delta\Delta C_T}$) method. All primer sequences are provided in Table S2.

2.8 Measurement of dopamine, IL-1β, IL6, TNF-α, and GLP-1 in serum

Dopamine (DA) levels in the substantia nigra (SN) and serum concentrations of IL-1β, IL6, TNF-α, and GLP-1 were quantified using commercial assay kits (Nanjing Jiancheng Bioengineering Institute, Nanjing, China, Cat. No. H170-1-2; 4A BIOTECH, Cat. Nos. CME0015, CME0006, and CME0004; and IBL, Tokyo, Japan, Cat. No. 27788) following the manufacturer's protocols. During sample collection, we did not use peptidase inhibitors (including dipeptidyl peptidase-4 (DPP-4) inhibitors), as our experimental design accounted for potential GLP-1 degradation by relying on sustained bacterial GLP-1 production to maintain stable levels.

2.9 Statistical analysis

Statistical analysis was performed using GraphPad Prism 7.0 (GraphPad Software, San Diego, CA, USA). Data were analyzed by one-way analysis of variance (ANOVA) with Tukey's post hoc test for multiple comparisons. Results are presented as mean±standard deviation (SD), and $P<0.05$ was considered statistically significant.

3 Results

3.1 Improvement of motor impairments in PD mice by *C. butyricum*-pMTL007-GLP-1

To assess the therapeutic effects of *C. butyricum*-pMTL007-GLP-1 in PD mice, we evaluated locomotor function through a series of behavioral tests (Fig. 1a). In the open-field test, PD mice showed characteristic deficits, including reduced center exploration time (anxious behavior), decreased total distance traveled (AM 1532 cm vs. C 3728 cm, $P<0.01$), and fewer center entries (AM 13.38 vs. C 30.00, $P<0.01$), all indicative of bradykinesia and impaired exploratory motivation. These impairments were substantially ameliorated by *C. butyricum*-pMTL007-GLP-1 treatment (ACBG), with efficacy comparable to liraglutide (Figs. 1b–1d). Motor-coordination assessments demonstrated parallel improvements, with ACBG normalizing both the prolonged pole-test descent time (ACBG 9.875 s vs. AM 15.790 s, $P<0.01$) and shortened hanging-test latency (ACBG 107.70 s vs. AM 50.33 s, $P<0.01$). Notably, ACBG outperformed the parental strain (ACB) in both tests (pole: 9.875 s vs. 12.920 s, $P<0.01$; hanging: 107.70 s vs. 78.10 s, $P<0.05$) while matching liraglutide's efficacy (Figs. 1e and 1f).

3.2 Restoration of disrupted gut microbiota in PD mice by *C. butyricum*-pMTL007-GLP-1

To investigate the effects of *C. butyricum*-pMTL007-GLP-1 on the gut microbiota composition in PD mice, we performed 16S rRNA high-throughput sequencing. Our findings demonstrated that α-diversity indices, including Chao1 and observed species richness, were significantly reduced in PD mice compared to control, but were partially restored following *C. butyricum*-pMTL007-GLP-1 treatment (Figs. 2a and 2b). Principal coordinate analysis (PCoA) based on unweighted UniFrac distances revealed distinct clustering patterns in the C and AM groups, with the ACBG group showing an intermediate microbial profile (Fig. 2c). Venn diagram analysis identified 320 OTUs shared across all groups, while the numbers of unique OTUs were 565 (C group), 339 (AM group), 437 (AL group), 419 (ACB group), and 492 (ACBG group) (Fig. 2d). Notably, the ACBG group exhibited the highest degree of OTU similarity with the C group, suggesting microbiota restoration. Taxonomic profiling at the phylum level showed that Bacteroidetes, Firmicutes, Proteobacteria, and Verrucomicrobia constituted the four most abundant phyla across all experimental groups (Fig. 2e). Notably, microbiome analysis revealed PD-associated dysbiosis marked by significant reduction in *Prevotella* ((2.5±1.0)% vs. control (6.1±2.0)%, $P<0.05$), a mucin-producing genus essential for gut-barrier integrity, and near elimination of the pro-inflammatory taxon *AF12* ((0.0±0.1)% vs. control (1.1±0.4)%, $P<0.05$). *C. butyricum*-pMTL007-GLP-1 treatment not only normalized but surpassed physiological *Prevotella* levels ((10±3)%, $P<0.05$) while restoring *AF12* to baseline ((1.0±0.2)%, $P<0.05$) (Figs. 2f–2j). These results demonstrate that *C. butyricum*-pMTL007-GLP-1 treatment can restore gut microbial diversity and composition in PD mice, potentially contributing to the observed therapeutic effects on PD symptoms.

3.3 Attenuation of intestinal α-synuclein accumulation and improvement of intestinal-barrier integrity in PD mice by *C. butyricum*-pMTL007-GLP-1

To assess the effects of *C. butyricum*-pMTL007-GLP-1 on intestinal pathophysiology in PD mice, we

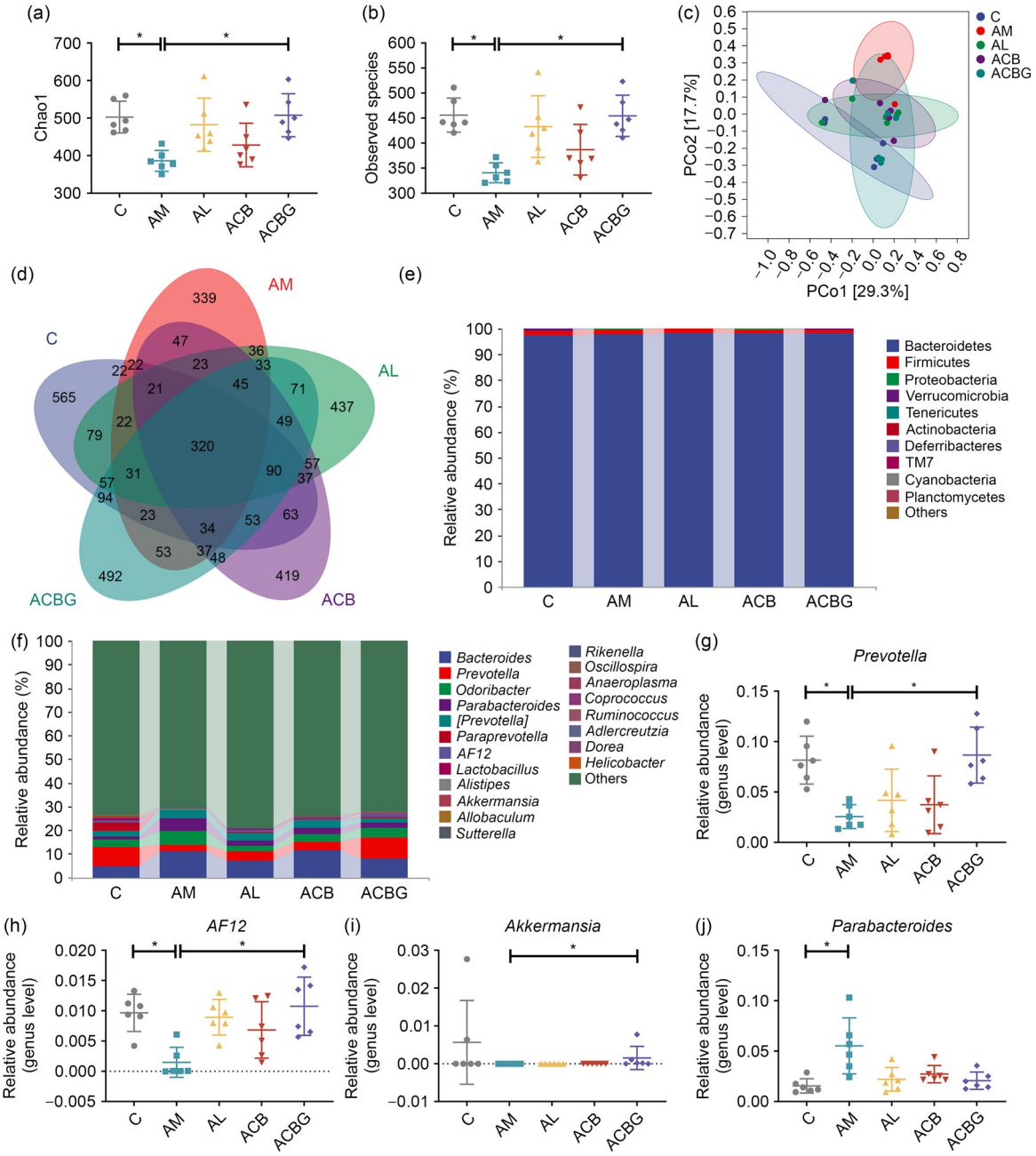

Fig. 2 Effect of *Clostridium butyricum*-pMTL007-glucagon-like peptide-1 (*C. butyricum*-pMTL007-GLP-1) on restored gut microbiota diversity in Parkinson's disease (PD) mice. (a) Chao1 index. (b) Observed species index. (c) Principal coordinate analysis (PCoA) plot of β-diversity index. (d) Venn diagram of operational taxonomic units (OTUs). (e) Microbial species composition at the phylum level. (f) Microbial species composition at the genus level. (g–j) Relative abundance of *Prevotella* (g), *AF12* (h), *Akkermansia* (i), and *Parabacteroides* (j). Data were analyzed by one-way analysis of variance (ANOVA) with Tukey's post hoc test for multiple comparisons. Data are presented as mean±standard deviation (SD). * *P*<0.05. C: normal mice (*n*=6); AM: PD mice (*n*=6); AL: liraglutide-treated PD mice (*n*=6); ACB: *C. butyricum*-treated PD mice (*n*=6); ACBG: *C. butyricum*-pMTL007-GLP-1-treated PD mice (*n*=6).

first examined GLP-1 secretion using immunofluorescence (IF). The AM group exhibited significantly lowe GLP-1 fluorescence intensity compared to the C group, while the *C. butyricum*-pMTL007-GLP-1 treatment substantially restored the fluorescence intensity (Figs. 3a and S1). We next evaluated α-syn pathology via immunohistochemistry (IHC). *C. butyricum*-pMTL007-GLP-1 treatment significantly reduced both

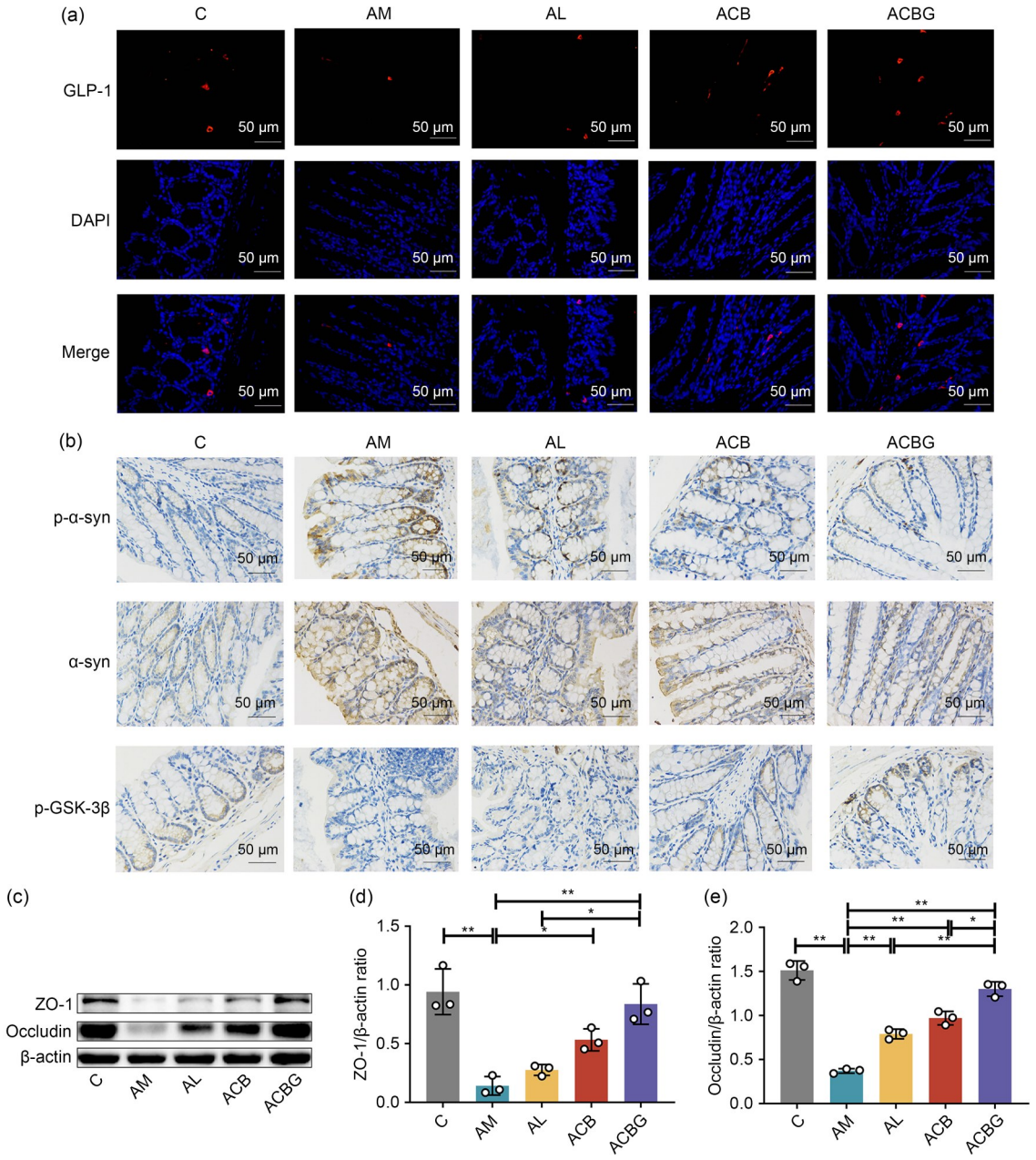

Fig. 3 Effects of *Clostridium butyricum*-pMTL007-glucagon-like peptide-1 (*C. butyricum*-pMTL007-GLP-1) reduced on intestinal α-synuclein (α-syn) expression and intestinal-barrier function by promoting GLP-1 secretion in Parkinson's disease (PD) mice. (a) Immunofluorescence analysis of GLP-1 in the colon. (b) Immunohistochemistry analysis of α-syn, phosphorylated-α-syn (p-α-syn), and p-glycogen synthase kinase-3β (p-GSK-3β) in the colon. (c–e) Western blot results showing expression of zonula occludens-1 (ZO-1) and occludin (with β-actin as the internal reference) in the colon. Data were analyzed by one-way analysis of variance (ANOVA) with Tukey's post hoc test for multiple comparisons. Data are presented as mean±standard deviation (SD). * P<0.05, ** P<0.01. C: normal mice (n=3); AM: PD mice (n=3); AL: liraglutide-treated PD mice (n=3); ACB: *C. butyricum*-treated PD mice (n=3); ACBG: *C. butyricum*-pMTL007-GLP-1-treated PD mice (n=3); DAPI: 4',6-diamidino-2-phenylindole dihydrochloride.

p-α-syn and α-syn accumulation while increasing p-GSK-3β levels in intestinal tissues (Fig. 3b). To investigate intestinal barrier function, we performed western blotting analysis of colonic tight-junction proteins. Compared to controls, PD mice showed markedly decreased expression of occludin and zonula occludens-1 (ZO-1), key components of intestinal tight junctions. Importantly, *C. butyricum*-pMTL007-GLP-1

treatment significantly restored the expression of these barrier proteins (Figs. 3c–3e). These results demonstrated that *C. butyricum*-pMTL007-GLP-1 exerted dual beneficial effects by reducing pathological α-syn accumulation in the gut and enhancing intestinal barrier integrity through GLP-1-mediated mechanisms. These findings suggest that the therapeutic effects of *C. butyricum*-pMTL007-GLP-1 on PD symptoms may be mediated, at least in this part, through gut–brain axis modulation.

3.4 Mitigation of neuropathological alterations in PD mice by *C. butyricum*-pMTL007-GLP-1

To evaluate dopaminergic neuron integrity, we first measured striatal DA levels by enzyme-linked immunosorbent assay (ELISA). PD mice exhibited significantly reduced DA content compared to controls (C vs. AM: 530.4 ng/mL vs. 405.9 ng/mL, $P<0.01$). Notably, all treatment groups showed substantial DA restoration (ACB: 479.5 ng/mL; AL: 488.8 ng/mL; ACBG: 520.9 ng/mL; all $P<0.01$ vs. AM), with *C. butyricum* (ACB) and *C. butyricum*-pMTL007-GLP-1 (ACBG) demonstrating efficacy comparable to liraglutide (Fig. 4a). Western blot analysis revealed concomitant changes in key dopaminergic markers. Both dopamine-transporter (DAT) and GLP-1-receptor (GLP-1R) expression levels were significantly downregulated in PD mice but restored following *C. butyricum*-pMTL007-GLP-1 treatment (Figs. 4b–4d). IF and immunoblotting further demonstrated that tyrosine hydroxylase (TH)-positive neurons, which were heavily depleted in PD mice, were significantly preserved across treatment groups, with maximal protection observed in the ACBG group (Figs. 4e and 4f). α-syn pathology analysis yielded complementary findings. Both p-α-syn and α-syn immunoreactivities were substantially increased in PD mice, but significantly attenuated by *C. butyricum*-pMTL007-GLP-1 treatment (Figs. 4g–4i and S1). Western blot quantification confirmed these morphological observations, showing reduced α-syn accumulation in the treated animals.

3.5 Attenuation of neuroinflammation and apoptosis via PI3K/AKT/GSK-3β pathway activation in PD mice by *C. butyricum*-pMTL007-GLP-1

To investigate the anti-neuroinflammatory effects of *C. butyricum*-pMTL007-GLP-1, we performed IF and western blot analyses to assess astrocyte initiation (glial fibrillary acidic protein (GFAP)) and microglia activation (ionized calcium-binding adapter molecule 1 (Iba1)) in the SN of A53T α-syn transgenic mice (Figs. 5a–5c). Quantitative analyses are presented in Fig. S1. Compared to the C group, the AM group displayed significant increases in both $GFAP^+$ astrocytes and $Iba1^+$ microglia in the SN ($P<0.01$). *C. butyricum*-pMTL007-GLP-1 treatment more potently attenuated glial activation than either liraglutide or wild-type *C. butyricum* alone, as confirmed by western blot quantification of GFAP and Iba1 protein levels. At the molecular level, qRT-PCR and ELISA analyses demonstrated elevated expression of pro-inflammatory cytokines (IL-1β, IL-6, and TNF-α) in PD mice, which were significantly suppressed by all treatments ($P<0.05$). The engineered probiotic (ACBG group) exhibited the most robust anti-inflammatory effects (Figs. 5a–5c). Importantly, *C. butyricum*-pMTL007-GLP-1 treatment also restored GLP-1R expression and increased GLP-1 levels (ACBG vs. AM: 8.068 pmol/L vs. 4.209 pmol/L, $P<0.01$; Fig. S1), suggesting a potential mechanism for its neuroprotective action.

To elucidate the molecular mechanisms underlying the anti-inflammatory effects of *C. butyricum*-pMTL007-GLP-1, we performed western blot analysis of the PI3K/AKT/GSK-3β signaling pathway in A53T α-syn transgenic mice (Figs. 5d–5h). Compared to the C group, the AM group demonstrated significant reductions in the phosphorylation ratios of PI3K (p-PI3K/PI3K), AKT (p-AKT/AKT), and GSK at $3\beta^{Ser9}$ (p-GSK-$3\beta^{Ser9}$/GSK-3β), along with elevated phosphorylation of p65 (p-p65/p65), indicative of NF-κB pathway activation (all $P<0.01$ vs. C group). Strikingly, *C. butyricum*-pMTL007-GLP-1 treatment not only normalized these aberrant signaling patterns but showed superior efficacy to both wild-type *C. butyricum* and liraglutide treatments. Further investigation of apoptotic regulators revealed that PD mice exhibited prominent dysregulation of apoptosis-related proteins, including increased expression of pro-apoptotic factors (B-cell lymphoma-2 (Bcl-2)-associated X protein (Bax) and cleaved-caspase-3) and reduced levels of anti-apoptotic Bcl-2 (Figs. 5i–5l). Treatment with *C. butyricum*-pMTL007-GLP-1 effectively restored the balance of these apoptotic markers, demonstrating comparable therapeutic effects to liraglutide ($P<0.05$ vs. AM group). Collectively, these findings suggest that *C. butyricum*-pMTL007-GLP-1 ameliorated PD pathology in A53T

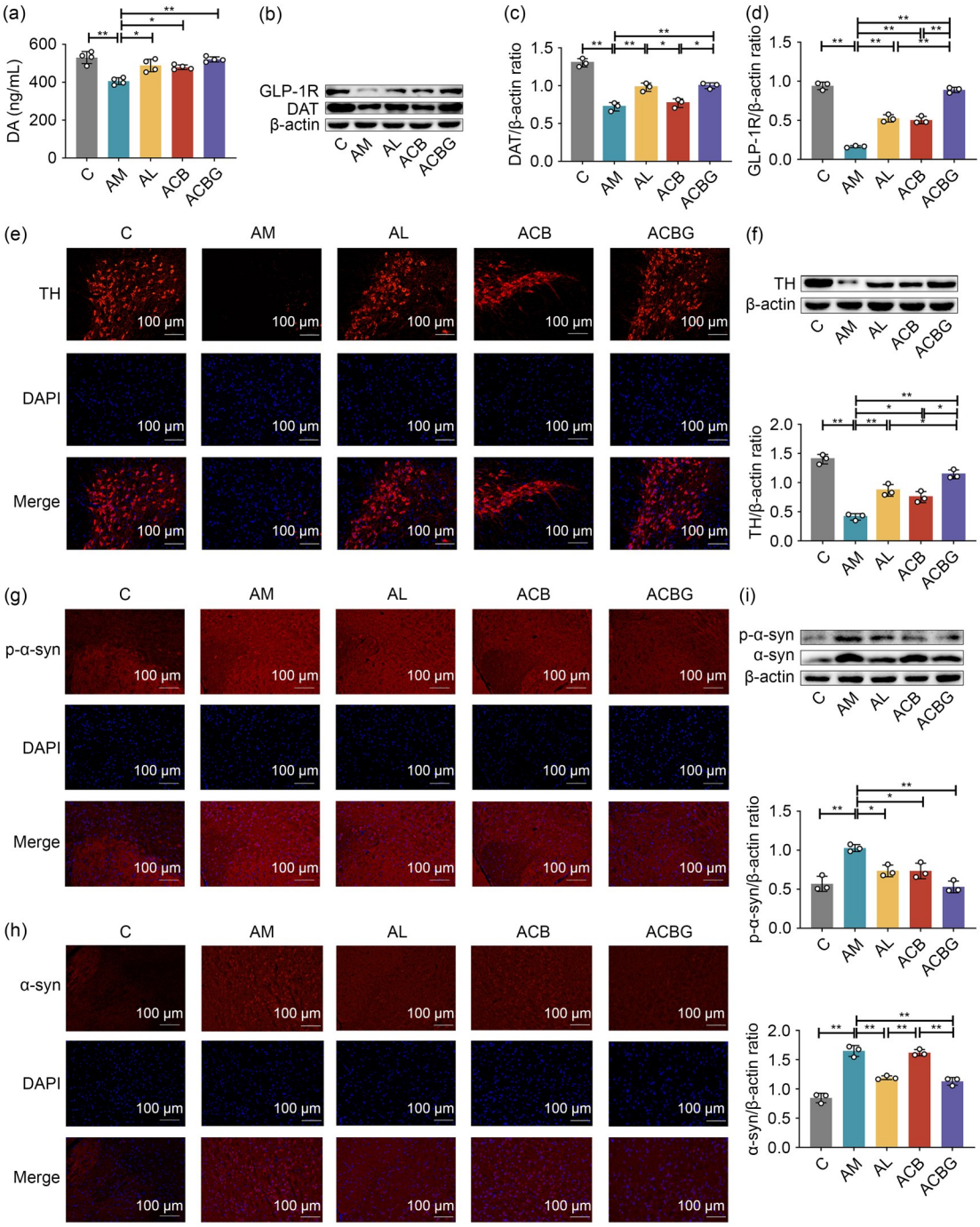

Fig. 4 Effect of *Clostridium butyricum*-pMTL007-glucagon-like peptide-1 (*C. butyricum*-pMTL007-GLP-1) on attenuated neuropathological variations in Parkinson's disease (PD) mice. (a) Expression levels of dopamine (DA) in the substantia nigra (SN) using enzyme-linked immunosorbent assay (ELISA) analysis (n=4). (b) Western blot results showing dopamine-transporter (DAT) and GLP-1 receptor (GLP-1R) expression (with β-actin as the internal reference) in the SN. (c, d) Quantitative analysis of DAT (c) and GLP-1R (d). (e, g, h) Immunofluorescence (IF) analyses of tyrosine hydroxylase (TH) (e), phosphorylated-α-synuclein (p-α-syn) (g), and α-syn (h). (f) Western blot analysis showing TH expression. (i) Western blot analysis showing p-α-syn and α-syn expression. Data were analyzed by one-way analysis of variance (ANOVA) with Tukey's post hoc test for multiple comparisons. Data are presented as mean±standard deviation (SD). * P<0.05, ** P<0.01. C: normal mice (n=3); AM: PD mice (n=3); AL: liraglutide-treated PD mice (n=3); ACB: *C. butyricum*-treated PD mice (n=3); ACBG: *C. butyricum*-pMTL007-GLP-1-treated PD mice (n=3); DAPI: 4',6-diamidino-2-phenylindole dihydrochloride.

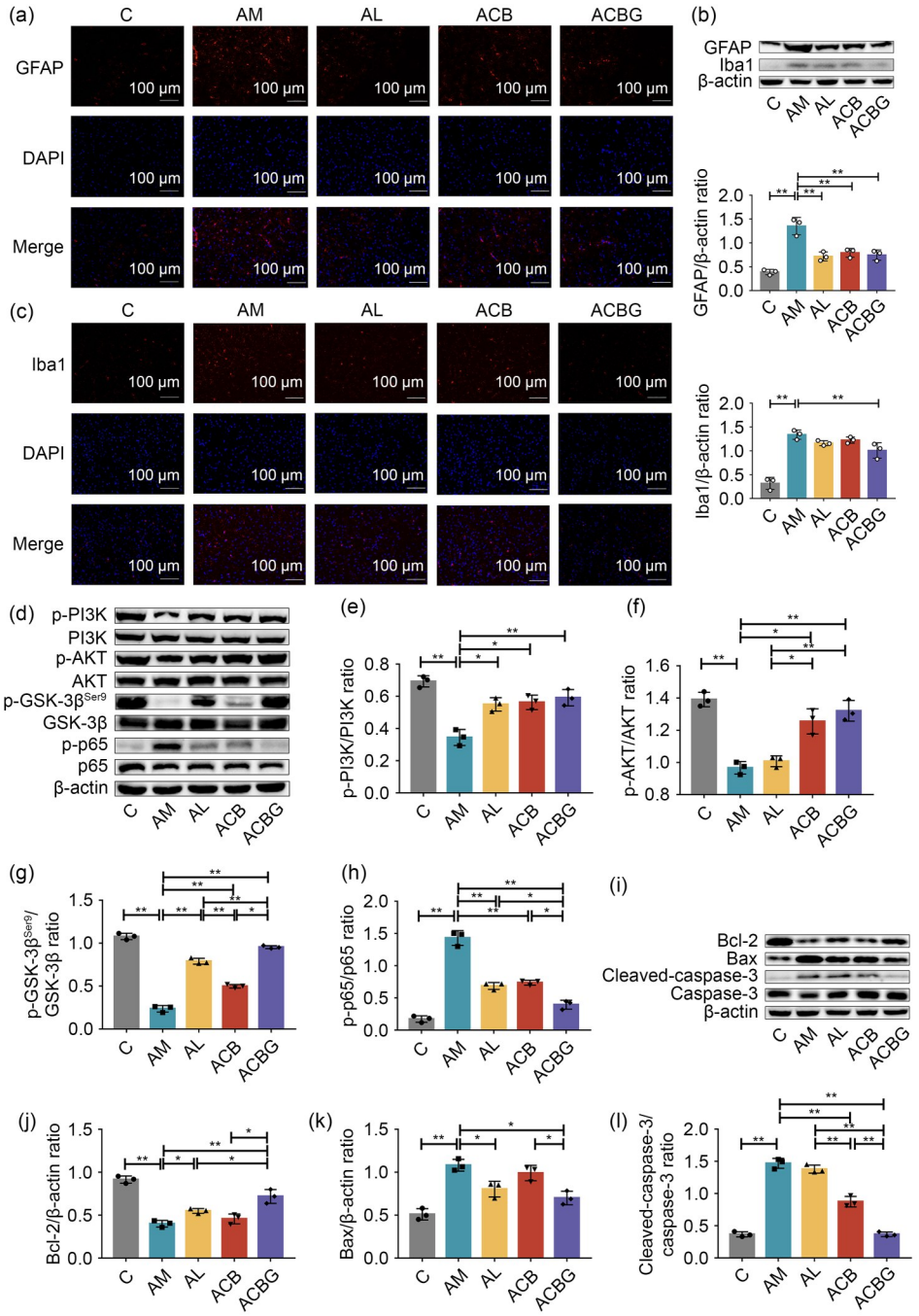

Fig. 5 Effect of *Clostridium butyricum*-pMTL007-glucagon-like peptide-1 (*C. butyricum*-pMTL007-GLP-1) on activated the phosphoinositide-3-kinase (PI3K)/protein kinase B (AKT)/glycogen synthase kinase-3β (GSK-3β) pathway to reduce inflammation and apoptosis in Parkinson's disease (PD) mice. (a, c) Immunofluorescence analyses of glial fibrillary acidic protein (GFAP) (a) and ionized calcium-binding adapter molecule 1 (Iba1) (c) in the substantia nigra (SN) of mice. (b) Western blot analysis showing GFAP, Iba1, and β-actin expression in the SN. (d) Western blot analysis showing protein expression of the signaling pathway. (e–h) Quantitative analysis of expression levels of phosphorylated PI3K (p-PI3K)/PI3K (e), p-AKT/AKT (f), p-GSK-3β^{Ser9}/GSK-3β (g), and p-p65/p65 (h). (i) Western blot analysis showing apoptosis-related protein expression. (j–l) Quantitative analysis of expression levels of B-cell lymphoma-2 (Bcl-2) (j), Bcl-2-associated X protein (Bax) (k), and cleaved-caspase-3/caspase-3 (l). Data were analyzed by one-way analysis of variance (ANOVA) with Tukey's post hoc test for multiple comparisons. Data are presented as mean±standard deviation (SD). * P<0.05, ** P<0.01. C: normal mice (n=3); AM: PD mice (n=3); AL: liraglutide-treated PD mice (n=3); ACB: *C. butyricum*-treated PD mice (n=3); ACBG: *C. butyricum*-pMTL007-GLP-1-treated PD mice (n=3); DAPI: 4',6-diamidino-2-phenylindole dihydrochloride.

α-syn transgenic mice through coordinated activation of the PI3K/AKT/GSK-3β neuroprotective pathway, which concurrently mediated potent anti-inflammatory effects and suppressed apoptotic signaling cascades.

4 Discussion

PD, the second most prevalent neurodegenerative disorder among middle-aged and elderly populations, remains without disease-modifying therapies to effectively halt its progression (Bohnen et al., 2025; Vaughan et al., 2025). Recent advances in microbiome research and genetic engineering technology have enabled the development of novel probiotic-based therapeutic strategies (Zommiti et al., 2020). Our research group has pioneered the development of three genetically engineered probiotic strains for sustained GLP-1 delivery: *L. lactis*-MG1363-pMG36e-GLP-1, *E. coli* Nissle 1917, and *C. butyricum*-pMTL007-GLP-1 (Fang et al., 2020; Wang et al., 2023). While all three strains demonstrated neuroprotective potential in PD models, the first two candidates (*L. lactis* and *E. coli*) present critical limitations such as antibiotic resistance markers, compromised gastrointestinal-tract viability, and formulation instability during storage. In contrast, *C. butyricum*-pMTL007-GLP-1 possesses distinct advantages due to its spore-forming capability, which confers remarkable stability during product storage while also maintaining therapeutic efficacy (Wang et al., 2023). The current study provides systematic evidence that *C. butyricum*-pMTL007-GLP-1 exerts substantial neuroprotective effects in PD mice through concurrent modulation of gut microbiota composition and activation of the PI3K/AKT/GSK-3β neuroprotective signaling pathway. These findings position *C. butyricum*-pMTL007-GLP-1 as a particularly promising translational candidate for PD intervention, combining microbial therapeutic benefits with enhanced pharmaceutical properties.

This study represents significant methodological and conceptual advancements over our previous work through several key innovations. First, while our prior research employed the MPTP-induced PD mouse model—which primarily reflects toxin-mediated dopaminergic neuron degeneration (Mosharov et al., 2009; Wang et al., 2011)—the current investigation employed the A53T α-syn transgenic mouse model, which more accurately recapitulates both the genetic and pathological hallmarks of human PD (Smidt et al., 2000; Graham and Sidhu, 2010; Xu et al., 2021). In addition, MPTP models, specifically those that are neurotoxin-induced, exhibit secondary gut dysfunction, such as reduced short-chain fatty acids (SCFAs) and mild dysbiosis, resulting from acute motor injury. Separately, A53T models, which are α-syn-transgenic, display primary gut pathology, including severe dysbiosis and 2-fold higher lipopolysaccharide (LPS) levels, due to early intestinal α-syn aggregation. These features better recapitulate PD's "gut-first" axis (Lai F et al., 2018; Liang et al., 2022). This strategic model selection substantially enhances the clinical relevance and translational potential of our findings. Second, we have significantly expanded the mechanistic understanding of *C. butyricum*-pMTL007-GLP-1's neuroprotective effects by comprehensively characterizing its activation of the PI3K/AKT/GSK-3β signaling cascade. Our results from this study demonstrate how this engineered probiotic concurrently mediates: (1) suppression of pro-inflammatory cytokine production, and (2) inhibition of apoptotic pathways through precise molecular regulation. These findings not only validate our previous observations of therapeutic potential but also provide a more rigorous, mechanism-based explanation for this probiotic's neuroprotective efficacy within a genetically relevant PD model.

Our experimental results reveal that A53T α-syn transgenic mice treated with *C. butyricum*-pMTL007-GLP-1 show significantly elevated GLP-1 levels in fecal samples and increased GLP-1-positive cell population in colonic tissues, confirming enhanced intestinal GLP-1 secretion. Mechanistically, the probiotic-induced GLP-1 upregulation appears to attenuate pathological α-syn aggregation through phosphorylation of GSK-3β at Ser9 (p-GSK-3β^{Ser9}), effectively reducing both α-syn phosphorylation and oligomerization (Su et al., 2022). This regulatory mechanism helps maintain proteostatic balance while preventing the accumulation of neurotoxic α-syn species. Considering the well-established fact that gut-derived α-syn is propagated to the central nervous system (Liptak et al., 2021; Liu et al., 2021), our data indicate that *C. butyricum*-pMTL007-GLP-1 exerts its therapeutic effects by suppressing colonic α-syn and p-α-syn aggregation through p-GSK-3β^{Ser9} activation, consequently improving intestinal-barrier integrity. By inhibiting α-syn

aggregation in the gut, this engineered probiotic may effectively block its pathological transmission along the gut–brain axis, potentially retarding PD progression. Importantly, the treatment clearly improved characteristic PD-like motor deficits in transgenic mice, including locomotor dysfunction, exploratory behavior impairment, muscle weakness, and balance-coordination deficits (Subbarayan et al., 2020). The comprehensive amelioration of both molecular pathologies and behavioral symptoms provides strong evidence for the neuroprotective efficacy of *C. butyricum*-pMTL007-GLP-1, highlighting its potential as a novel disease-modifying therapy for PD that targets both symptom management and underlying disease progression.

Expanding upon previous findings that demonstrate the efficacy of engineered *C. butyricum*-pMTL007-GLP-1 in modulating gut microbiota composition in MPTP-induced PD rodent models (Wang et al., 2023), we investigated its therapeutic potential in A53T α-syn transgenic mice, a genetically relevant PD model. Our results confirm that this engineered probiotic not only restores intestinal microbial diversity but specifically increases the relative abundance of *Prevotella*, a bacterial genus consistently shown to be depleted in both clinical PD population and preclinical models (Lin et al., 2019). *AF12*, which is typically pro-inflammatory, disappears in PD mice but partially recovers after probiotic treatment, suggesting that PD creates a hostile gut environment. Engineered probiotics promote their non-pathogenic repopulation—a balanced state that is potentially vital for microbiome function and also consistent with reported benefits in metabolism and gut barrier integrity (Lai ZL et al., 2018; Zhao et al., 2020). These findings significantly extend previous work by demonstrating the microbiota-modulating effects of *C. butyricum*-pMTL007-GLP-1 across distinct PD models while validating *Prevotella* as a key microbial marker associated with PD pathology.

The critical involvement of neuroinflammatory mechanisms in PD pathogenesis has been well documented (Tansey and Goldberg, 2010; Wang et al., 2015). Here, we systematically evaluated the anti-neuroinflammatory effects of engineered *C. butyricum*-pMTL007-GLP-1 in PD mouse models. In a study by Rojo et al. (2010), IF and western blotting analyses revealed marked upregulation of glial activation markers (GFAP and Iba1) in PD mice, which was significantly attenuated by *C. butyricum*-pMTL007-GLP-1 treatment. According to Yan et al. (2014), the engineered probiotic also effectively suppresses key pro-inflammatory cytokines (IL-1β, IL-6, and TNF-α), demonstrating potent anti-inflammatory activity. Mechanistically, we identified that GLP-1R activation by the engineered bacteria initiates PI3K/AKT signaling, as evidenced by increased p-PI3K and p-AKT levels coupled with reduced p-p65 expression in brain tissues (Cui et al., 2016; Yao et al., 2021). Furthermore, we observed enhanced phosphorylation of GSK-3β at Ser9, a crucial downstream effector of PI3K/AKT signaling known to counteract both inflammatory and apoptotic pathways (Credle et al., 2015). Together, these findings establish that *C. butyricum*-pMTL007-GLP-1 exerts neuroprotective effects in PD through multifaceted mechanisms involving suppression of neuroinflammation, inhibition of apoptotic signaling, and promotion of neuronal survival via the PI3K/AKT/GSK-3β axis.

While this study provides compelling evidence for the neuroprotective effects of engineered *C. butyricum*-pMTL007-GLP-1 in PD mouse models, several limitations should be acknowledged. First, although we identified the PI3K/AKT/GSK-3β pathway as a key mediator of the probiotic's anti-inflammatory and anti-apoptotic effects, the precise molecular interactions between GLP-1R activation and downstream signaling remain incompletely elucidated. Second, while gut microbiota modulation was observed, the direct contribution of specific bacterial taxa (e.g., *Prevotella*) to neuroprotection remains speculative. Finally, the long-term safety and efficacy of engineered probiotics in PD treatment remain unexplored.

5 Conclusions

In summary, our findings demonstrate that *C. butyricum*-pMTL007-GLP-1 exerts comprehensive neuroprotective effects in PD mice through multiple synergistic mechanisms: (1) amelioration of motor dysfunction via reduction of α-syn expression and enhancement of intestinal-barrier integrity; (2) restoration of gut microbial homeostasis, including normalization of *Prevotella* abundance; and (3) attenuation of neuropathological changes through decreased nigral p-α-syn accumulation and upregulation of TH, DAT, and GLP-1R expression. These therapeutic benefits

are mediated through coordinated suppression of pro-inflammatory cytokines and activation of the PI3K/AKT/GSK-3β signaling cascade, which concurrently inhibits neuroinflammatory responses and promotes neuronal survival. Collectively, our results provide compelling preclinical evidence supporting *C. butyricum*-pMTL007-GLP-1 as a promising multifactorial therapeutic strategy for PD, targeting both gastrointestinal and central nervous-system pathologies through gut–brain-axis modulation.

Data availability statement

The datasets analyzed in this study are available from the corresponding author upon reasonable request. Raw sequences have been deposited in the GenBank database (Accession No. PRJNA 1091924).

Acknowledgments

This work was supported by the Jiangxi Provincial Natural Science Foundation (Nos. 20242BAB26134 and 20242BAB25464), the Academic and Technical Leaders of Major Disciplines in Jiangxi Province (No. 20213BCJL22049), and the National Natural Science Foundation of China (Nos. 82060222 and 82460237).

Author contributions

Xin FANG conceived the study, designed the methodology, and provided financial support. Yun WANG developed the methodology, performed formal analysis, and wrote the original draft. Zhenli LONG, Bin LIAO, Bo WANG, and Daojun HONG conducted the investigations and data curation. Jie LUO secured funding, supervised the project, and contributed to manuscript revisions. Tingtao CHEN conceptualized the study, provided supervision, and acquired funding. All authors have read and approved the final manuscript, and therefore, have full access to all the data in the study and take responsibility for the integrity and security of the data.

Compliance with ethics guidelines

Xin FANG, Yun WANG, Zhenli LONG, Bin LIAO, Bo WANG, Daojun HONG, Jie LUO, and Tingtao CHEN declare that they have no conflicts of interest.

Animal care protocols and all experimental procedures adhered to National Institutes of Health guidelines and were approved by the Animal Experimental Ethical Inspection Committee of Nanchang Royo Biotechnology Co., Ltd., Nanchang, China (Approval No. RyE2021070912).

Declaration on the use of generative AI tools

During the preparation of this work, the authors used Deepseek to improve the language fluency and check grammatical errors. After using this tool, the authors reviewed and edited the content as needed and take full responsibility for the content of the publication.

References

Bohnen NI, Roytman S, van der Zee S, et al., 2025. A multicenter longitudinal study of cholinergic subgroups in Parkinson disease. *Nat Commun*, 16:5655. https://doi.org/10.1038/s41467-025-60815-0

Chang EES, Ho PWL, Liu HF, et al., 2022. *LRRK2* mutant knockin mouse models: therapeutic relevance in Parkinson's disease. *Transl Neurodegener*, 11:10. https://doi.org/10.1186/s40035-022-00285-2

Chen TT, Tian PY, Huang ZX, et al., 2018. Engineered commensal bacteria prevent systemic inflammation-induced memory impairment and amyloidogenesis via producing GLP-1. *Appl Microbiol Biotechnol*, 102(17):7565-7575. https://doi.org/10.1007/s00253-018-9155-6

Chidambaram SB, Essa MM, Rathipriya AG, et al., 2022. Gut dysbiosis, defective autophagy and altered immune responses in neurodegenerative diseases: tales of a vicious cycle. *Pharmacol Ther*, 231:107988. https://doi.org/10.1016/j.pharmthera.2021.107988

Credle JJ, George JL, Wills J, et al., 2015. GSK-3*β* dysregulation contributes to Parkinson's-like pathophysiology with associated region-specific phosphorylation and accumulation of Tau and *α*-synuclein. *Cell Death Differ*, 22(5):838-851. https://doi.org/10.1038/cdd.2014.179

Cui C, Cui NS, Wang P, et al., 2016. Neuroprotective effect of sulfated polysaccharide isolated from sea cucumber *Stichopus japonicus* on 6-OHDA-induced death in SH-SY5Y through inhibition of MAPK and NF-κB and activation of PI3K/Akt signaling pathways. *Biochem Biophys Res Commun*, 470(2):375-383. https://doi.org/10.1016/j.bbrc.2016.01.035

Fang X, Zhou XT, Miao YQ, et al., 2020. Therapeutic effect of GLP-1 engineered strain on mice model of Alzheimer's disease and Parkinson's disease. *AMB Express*, 10:80. https://doi.org/10.1186/s13568-020-01014-6

Golpich M, Amini E, Hemmati F, et al., 2015. Glycogen synthase kinase-3 beta (GSK-3β) signaling: implications for Parkinson's disease. *Pharmacol Res*, 97:16-26. https://doi.org/10.1016/j.phrs.2015.03.010

Gowayed MA, El-Sayed NS, Matar NA, et al., 2022. The α7 nAChR allosteric modulator PNU-120596 amends neuroinflammatory and motor consequences of parkinsonism in rats: role of JAK2/NF-κB/GSk3β/TNF-α pathway. *Biomed Pharmacother*, 148:112776. https://doi.org/10.1016/j.biopha.2022.112776

Graham DR, Sidhu A, 2010. Mice expressing the A53T mutant form of human alpha-synuclein exhibit hyperactivity and reduced anxiety-like behavior. *J Neurosci Res*, 88(8):1777-1783. https://doi.org/10.1002/jnr.22331

Higashi S, Biskup S, West AB, et al., 2007. Localization of Parkinson's disease-associated LRRK2 in normal and pathological human brain. *Brain Res*, 1155:208-219. https://doi.org/10.1016/j.brainres.2007.04.034

Hölscher C, 2018. Novel dual GLP-1/GIP receptor agonists show neuroprotective effects in Alzheimer's and Parkinson's disease models. *Neuropharmacology*, 136:251-259. https://doi.org/10.1016/j.neuropharm.2018.01.040

Holst JJ, 2007. The physiology of glucagon-like peptide 1. *Physiol Rev*, 87(4):1409-1439. https://doi.org/10.1152/physrev.00034.2006

Kozikowski AP, Gaisina IN, Petukhov PA, et al., 2006. Highly potent and specific GSK-3β inhibitors that block Tau phosphorylation and decrease α-synuclein protein expression in a cellular model of Parkinson's disease. *ChemMedChem*, 1(2):256-266. https://doi.org/10.1002/cmdc.200500039

Lai F, Jiang R, Xie WJ, et al., 2018. Intestinal pathology and gut microbiota alterations in a methyl-4-phenyl-1,2,3,6-tetrahydropyridine (MPTP) mouse model of Parkinson's disease. *Neurochem Res*, 43(10):1986-1999. https://doi.org/10.1007/s11064-018-2620-x

Lai ZL, Tseng CH, Ho HJ, et al., 2018. Fecal microbiota transplantation confers beneficial metabolic effects of diet and exercise on diet-induced obese mice. *Sci Rep*, 8: 15625. https://doi.org/10.1038/s41598-018-33893-y

Lei P, Ayton S, Bush AI, et al., 2011. GSK-3 in neurodegenerative diseases. *Int J Alzheimers Dis*, 2011:189246. https://doi.org/10.4061/2011/189246

Liang F, Chen CY, Li YP, et al., 2022. Early dysbiosis and dampened gut microbe oscillation precede motor dysfunction and neuropathology in animal models of Parkinson's disease. *J Parkinsons Dis*, 12(8):2423-2440. https://doi.org/10.3233/JPD-223431

Lin CH, Chen CC, Chiang HL, et al., 2019. Altered gut microbiota and inflammatory cytokine responses in patients with Parkinson's disease. *J Neuroinflammation*, 16:129. https://doi.org/10.1186/s12974-019-1528-y

Liptak R, Gromova B, Gardlik R, 2021. Fecal microbiota transplantation as a tool for therapeutic modulation of non-gastrointestinal disorders. *Front Med*, 8:665520. https://doi.org/10.3389/fmed.2021.665520

Liu ML, Fan GH, Meng LK, et al., 2025. New perspectives on microbiome-dependent gut-brain pathways for the treatment of depression with gastrointestinal symptoms: from bench to bedside. *J Zhejiang Univ-Sci B (Biomed & Biotechnol)*, 26(1):1-25. https://doi.org/10.1631/jzus.B2300343

Liu XR, Liu SY, Tang Y, et al., 2021. Intragastric administration of casein leads to nigrostriatal disease progressed accompanied with persistent nigrostriatal-intestinal inflammation activited and intestinal microbiota-metabolic disorders induced in MPTP mouse model of Parkinson's disease. *Neurochem Res*, 46(6):1514-1539. https://doi.org/10.1007/s11064-021-03293-2

Lorenz M, Evers A, Wagner M, 2013. Recent progress and future options in the development of GLP-1 receptor agonists for the treatment of diabesity. *Bioorg Med Chem Lett*, 23(14):4011-4018. https://doi.org/10.1016/j.bmcl.2013.05.022

Lv LL, Tan XL, Peng XK, et al., 2020. The relationships of vitamin D, vitamin D receptor gene polymorphisms, and vitamin D supplementation with Parkinson's disease. *Transl Neurodegener*, 9:34. https://doi.org/10.1186/s40035-020-00213-2

Malagelada C, Jin ZH, Greene LA, 2008. RTP801 is induced in Parkinson's disease and mediates neuron death by inhibiting Akt phosphorylation/activation. *J Neurosci*, 28(53): 14363-14371. https://doi.org/10.1523/JNEUROSCI.3928-08.2008

Meng JR, Ma X, Wang N, et al., 2016. Activation of GLP-1 receptor promotes bone marrow stromal cell osteogenic differentiation through β-catenin. *Stem Cell Rep*, 6(4): 579-591. https://doi.org/10.1016/j.stemcr.2016.02.002

Mosharov EV, Larsen KE, Kanter E, et al., 2009. Interplay between cytosolic dopamine, calcium, and α-synuclein causes selective death of substantia nigra neurons. *Neuron*, 62(2):218-229. https://doi.org/10.1016/j.neuron.2009.01.033

Mulvaney CA, Duarte GS, Handley J, et al., 2020. GLP-1 receptor agonists for Parkinson's disease. *Cochrane Database Syst Rev*, 7(7):CD012990. https://doi.org/10.1002/14651858.CD012990.pub2

Reich N, Hölscher C, 2022. The neuroprotective effects of glucagon-like peptide 1 in Alzheimer's and Parkinson's disease: an in-depth review. *Front Neurosci*, 16:970925. https://doi.org/10.3389/fnins.2022.970925

Rojo AI, Innamorato NG, Martín-Moreno AM, et al., 2010. Nrf2 regulates microglial dynamics and neuroinflammation in experimental Parkinson's disease. *Glia*, 58(5):588-598. https://doi.org/10.1002/glia.20947

Sharma N, Soni R, Sharma M, et al., 2022. Chlorogenic acid: a polyphenol from coffee rendered neuroprotection against rotenone-induced Parkinson's disease by GLP-1 secretion. *Mol Neurobiol*, 59(11):6834-6856. https://doi.org/10.1007/s12035-022-03005-z

Smidt MP, Asbreuk CHJ, Cox JJ, et al., 2000. A second independent pathway for development of mesencephalic dopaminergic neurons requires *Lmx1b*. *Nat Neurosci*, 3(4): 337-341. https://doi.org/10.1038/73902

Snigdha S, Ha K, Tsai P, et al., 2022. Probiotics: potential novel therapeutics for microbiota-gut-brain axis dysfunction across gender and lifespan. *Pharmacol Ther*, 231: 107978. https://doi.org/10.1016/j.pharmthera.2021.107978

Stoeva MK, Garcia-So J, Justice N, et al., 2021. Butyrate-producing human gut symbiont, *Clostridium butyricum*, and its role in health and disease. *Gut Microbes*, 13(1): 1907272. https://doi.org/10.1080/19490976.2021.1907272

Su YF, Liu NN, Zhang ZJ, et al., 2022. Cholecystokinin and glucagon-like peptide-1 analogues regulate intestinal tight junction, inflammation, dopaminergic neurons and α-synuclein accumulation in the colon of two Parkinson's disease mouse models. *Eur J Pharmacol*, 926:175029.

https://doi.org/10.1016/j.ejphar.2022.175029

Subbarayan MS, Hudson C, Moss LD, et al., 2020. T cell infiltration and upregulation of MHC II in microglia leads to accelerated neuronal loss in an α-synuclein rat model of Parkinson's disease. *J Neuroinflammation*, 17:242. https://doi.org/10.1186/s12974-020-01911-4

Sun J, Li HJ, Jin YJ, et al., 2021. Probiotic *Clostridium butyricum* ameliorated motor deficits in a mouse model of Parkinson's disease via gut microbiota-GLP-1 pathway. *Brain Behav Immun*, 91:703-715. https://doi.org/10.1016/j.bbi.2020.10.014

Tansey MG, Goldberg MS, 2010. Neuroinflammation in Parkinson's disease: its role in neuronal death and implications for therapeutic intervention. *Neurobiol Dis*, 37(3): 510-518. https://doi.org/10.1016/j.nbd.2009.11.004

Tarsy D, 2012. Treatment of Parkinson disease: a 64-year-old man with motor complications of advanced Parkinson disease. *JAMA*, 307(21):2305-2314. https://doi.org/10.1001/jama.2012.4829

Tripodi F, Lambiase A, Moukham H, et al., 2024. Targeting protein aggregation using a cocoa-bean shell extract to reduce α-synuclein toxicity in models of Parkinson's disease. *Curr Res Food Sci*, 9:100888. https://doi.org/10.1016/j.crfs.2024.100888

Vaughan CP, Morley JF, Lehosit J, et al., 2025. Behavioral compared with drug therapy for overactive bladder symptoms in Parkinson disease: a randomized noninferiority trial. *JAMA Neurol*, 14:e251904. https://doi.org/10.1001/jamaneurol.2025.1904

Wang Q, Luo YQ, Ray Chaudhuri K, et al., 2021. The role of gut dysbiosis in Parkinson's disease: mechanistic insights and therapeutic options. *Brain*, 144(9):2571-2593. https://doi.org/10.1093/brain/awab156

Wang QQ, Liu YJ, Zhou JW, 2015. Neuroinflammation in Parkinson's disease and its potential as therapeutic target. *Transl Neurodegener*, 4:19. https://doi.org/10.1186/s40035-015-0042-0

Wang Y, Chen S, Xu Z, et al., 2018. GLP-1 receptor agonists downregulate aberrant GnT-III expression in Alzheimer's disease models through the Akt/GSK-3β/β-catenin signaling. *Neuropharmacology*, 131:190-199. https://doi.org/10.1016/j.neuropharm.2017.11.048

Wang Y, Chen WJ, Han YY, et al., 2023. Neuroprotective effect of engineered *Clostridium butyricum*-pMTL007-GLP-1 on Parkinson's disease mice models via promoting mitophagy. *Bioeng Transl Med*, 8(3):e10505. https://doi.org/10.1002/btm2.10505

Wang ZQ, Zhang Y, Zhang S, et al., 2011. DJ-1 can inhibit microtubule associated protein 1 B formed aggregates. *Mol Neurodegener*, 6:38. https://doi.org/10.1186/1750-1326-6-38

Wu H, Wei J, Zhao XM, et al., 2023. Neuroprotective effects of an engineered *Escherichia coli* Nissle 1917 on Parkinson's disease in mice by delivering GLP-1 and modulating gut microbiota. *Bioeng Transl Med*, 8(5):e10351. https://doi.org/10.1002/btm2.10351

Wu X, Li S, Xue P, et al., 2018. Liraglutide inhibits the apoptosis of MC3T3-E1 cells induced by serum deprivation through cAMP/PKA/β-catenin and PI3K/AKT/GSK3β signaling pathways. *Mol Cells*, 41(3):234-243. https://doi.org/10.14348/molcells.2018.2340

Xu WX, Qi YZ, Gao YJ, et al., 2021. Benzo(*a*)pyrene exposure in utero exacerbates Parkinson's Disease (PD)-like α-synucleinopathy in A53T human alpha-synuclein transgenic mice. *Toxicol Appl Pharmacol*, 427:115658. https://doi.org/10.1016/j.taap.2021.115658

Xu X, Xu TC, Wei J, et al., 2024. Gut microbiota: an ideal biomarker and intervention strategy for aging. *Microbiome Res Rep*, 3(2):13. https://doi.org/10.20517/mrr.2023.68

Yan JQ, Fu QZ, Cheng LN, et al., 2014. Inflammatory response in Parkinson's disease (Review). *Mol Med Rep*, 10(5): 2223-2233. https://doi.org/10.3892/mmr.2014.2563

Yang JCS, Wu SC, Rau CS, et al., 2014. Inhibition of the phosphoinositide 3-kinase pathway decreases innate resistance to lipopolysaccharide toxicity in TLR4 deficient mice. *J Biomed Sci*, 21:20. https://doi.org/10.1186/1423-0127-21-20

Yang JL, Chen WY, Chen YP, et al., 2016. Activation of GLP-1 receptor enhances neuronal base excision repair via PI3K-AKT-induced expression of apurinic/apyrimidinic endonuclease 1. *Theranostics*, 6(12):2015-2027. https://doi.org/10.7150/thno.15993

Yao MY, Zhang J, Li ZH, et al., 2021. Liraglutide protects nucleus pulposus cells against high-glucose induced apoptosis by activating PI3K/Akt/mTOR/caspase-3 and PI3K/Akt/GSK3β/caspase-3 signaling pathways. *Front Med*, 8: 630962. https://doi.org/10.3389/fmed.2021.630962

Zeng CY, Chen TT, Zhang Y, et al., 2017. Hedgehog signaling pathway regulates ovarian cancer invasion and migration via adhesion molecule CD24. *J Cancer*, 8(5):786-792. https://doi.org/10.7150/jca.17712

Zhang YC, Bailey TS, Hittmeyer P, et al., 2024. Multiplex genetic manipulations in *Clostridium butyricum* and *Clostridium sporogenes* to secrete recombinant antigen proteins for oral-spore vaccination. *Microb Cell Fact*, 23:119. https://doi.org/10.1186/s12934-024-02389-y

Zhao BT, Xia B, Li XH, et al., 2020. Sesamol supplementation attenuates DSS-induced colitis via mediating gut barrier integrity, inflammatory responses, and reshaping gut microbiome. *J Agric Food Chem*, 68(39):10697-10708. https://doi.org/10.1021/acs.jafc.0c04370

Zommiti M, Feuilloley MGJ, Connil N, 2020. Update of probiotics in human world: a nonstop source of benefactions till the end of time. *Microorganisms*, 8(12):1907. https://doi.org/10.3390/microorganisms8121907

Supplementary information

Tables S1 and S2; Fig. S1